

OPEN
ARTICLE

qMRI-BIDS: An extension to the brain imaging data structure for quantitative magnetic resonance imaging data

Agah Karakuzu^{1,2} , Stefan Appelhoff³ , Tibor Auer⁴ , Mathieu Boudreau^{1,2}, Franklin Feingold⁵ , Ali R. Khan⁶ , Alberto Lazari⁷ , Chris Markiewicz⁵ , Martijn Mulder⁸, Christophe Phillips⁹ , Taylor Salo¹⁰ , Nikola Stikov^{1,2,11}, Kirstie Whitaker¹²  & Gilles de Hollander^{13,14} 

The Brain Imaging Data Structure (BIDS) established community consensus on the organization of data and metadata for several neuroimaging modalities. Traditionally, BIDS had a strong focus on functional magnetic resonance imaging (fMRI) datasets and lacked guidance on how to store *multimodal* structural MRI datasets. Here, we present and describe the BIDS Extension Proposal 001 (BEP001), which adds a range of quantitative MRI (qMRI) applications to the BIDS. In general, the aim of qMRI is to characterize brain microstructure by quantifying the physical MR parameters of the tissue via computational, biophysical models. By proposing this new standard, we envision standardization of qMRI through multicenter dissemination of interoperable datasets. This way, BIDS can act as a catalyst of convergence between qMRI methods development and application-driven neuroimaging studies that can help develop quantitative biomarkers for neural tissue characterization. In conclusion, this BIDS extension offers a common ground for developers to exchange novel imaging data and tools, reducing the entrance barrier for qMRI in the field of neuroimaging.

Introduction

The brain imaging data structure (BIDS) is an open-source initiative from the neuroimaging community that aids in standardizing neuroimaging data sets. BIDS was originally developed with functional MRI (fMRI) applications in mind, describing experimental task blocks in relation to a hierarchical organization of reconstructed MR images¹. This convention engaged researchers to share hundreds of open fMRI data on the openneuro platform^{2,3} and to develop interoperable processing workflows that can seamlessly process these datasets⁴. Popular examples include the MRIQC⁵ and fmripip⁶ pipelines, which can be executed online for any valid BIDS fMRI dataset. Similarly, the development of an MRI k-space data standard, ISMRM-RD⁷, led open-source MRI reconstruction packages to adapt this convention and now aids potential users in performing advanced reconstruction tasks with minimal effort^{8,9}. These success stories from open science exemplify how data standards can

¹NeuroPoly Lab, Institute of Biomedical Engineering, Polytechnique Montreal, Montréal, QC, Canada. ²Montreal Heart Institute, Montreal, QC, Canada. ³Center for Adaptive Rationality, Max Planck Institute for Human Development, Berlin, Germany. ⁴NeuroModulation Lab, School of Psychology, University of Surrey, Guildford, UK. ⁵Stanford University, Stanford, CA, USA. ⁶Department of Medical Biophysics, Robarts Research Institute, University of Western Ontario, London, Canada. ⁷Wellcome Centre for Integrative Neuroimaging, FMRIB, Nuffield Department of Clinical Neurosciences, University of Oxford, Oxford, UK. ⁸Department of Experimental Psychology, Utrecht University, Utrecht, the Netherlands. ⁹GIGA Cyclotron Research Centre in vivo imaging, GIGA Institute, University of Liège, Liège, Belgium. ¹⁰Florida International University, Miami, FL, USA. ¹¹Center for Advanced Interdisciplinary Research, Ss. Cyril and Methodius University, Skopje, North Macedonia. ¹²The Alan Turing Institute, London, UK. ¹³Zurich Center for Neuroeconomics (ZNE), Department of Economics, University of Zurich, Zurich, Switzerland. ¹⁴Spinoza Centre for Neuroimaging, Amsterdam, The Netherlands. ✉e-mail: agahkarakuzu@gmail.com; kwhitaker@turing.ac.uk; gilles.de.hollander@gmail.com

change the landscape of community-driven software for the better, leading to a collective change in researchers' behaviour to adhere with FAIR (findability, accessibility, interoperability and reusability) principles of scientific data¹⁰. Here we present our work extending the BIDS to include multi-contrast MRI acquisitions for quantitative MRI (qMRI) applications.

Quantitative MRI methods map physical properties of the (brain) tissue. These techniques consist of two steps: i) collecting multiple MRI images, where the contributions of effective micrometer-level MRI parameters is systematically manipulated by adapting very specific acquisition parameters, and ii) fitting the resultant voxel intensity variations across the images to a computational (biophysical) model¹¹. The results are a single or multiple quantitative *maps* of the estimated parameters across the imaged volume. The effective MRI parameters that are typically studied include longitudinal and transverse relaxation time constants (T1 and T2, respectively), proton density (PD), magnetization transfer (MT), and local diffusion coefficient (e.g., fractional anisotropy, FA, or mean diffusivity, MD). Another important technique used in qMRI is field mapping, which characterizes inhomogeneities in MRI radiofrequency (RF) transmit (B1+) and receive (B1-) profiles, as well as static magnetic field (B0) to correct qMRI parameter estimation errors for these field inhomogeneities.

The earliest qMRI applications date back to the late 70s¹² and primarily focused on relaxometry, i.e., mapping of quantities such as T1 and T2* relaxation time. Since then, the field has witnessed multiple waves of methods development, driven by technological advances and emerging trends in MRI research^{13,14}. Recently, with the surge of deep learning methods, the gamut of parameter estimation methods has become much larger than ever before^{14–18}. Interestingly, however, the healthy range of relaxation time values is still not known for multi-center studies¹⁹. This discrepancy highlights that multicenter standardization should be a critical step toward evaluating the clinical potential of decades-long improvements in the acquisition and processing of qMRI data.

Under more controlled research settings, qMRI offers obvious advantages over conventional MRI contrasts (e.g., T1 weighted images) in structural feature extraction. Given that MRI is not a direct measurement of *in vivo* anatomical structures, voxel-wise morphometry analyses are subjected to various biochemical and physiological confounders affecting the voxel intensity²⁰. Hence, the capacity of disentangling MRI signal components lends qMRI as a more reliable approach to study structural variations²¹. This makes qMRI a powerful tool for comparisons of the brain anatomy of different (clinical) groups^{22–24} and for more consistent, unbiased automated anatomical segmentation^{25–28}. The same principle can be exploited to make qMRI sensitive to tissue microstructure, such as iron concentration or myelination. Recent meta analyses revealed that a majority of qMRI methods are comparably sensitive to the myelin content^{29,30}, although certain parameters such as myelin water fraction (MWF, relaxometry-based) and macromolecular pool fraction (MPF, MT-based) appear to be more specific.

Given the advantages offered by parametric maps in providing structural information and the current landscape of myelin imaging methods, it seems likely that more myelin imaging methods leveraging the potential of qMRI will be developed in the future. This leads to one of our four main motivations behind covering qMRI methods in BIDS: to bring FAIR principles to a variety of qMRI data that are finding widespread use in neuroimaging research. Other motivations include i) driving open-source qMRI tools to adapt a consolidated input/output convention, ii) creating standardized databases that can help simplify the use of qMRI in clinical and translational research, and iii) stimulating an open provision of qMRI data that can be collected by imaging equipment that is available to a small group of researchers.

Drawing upon the principles outlined in BIDS, we introduce the first consensus data and metadata organization standard for qMRI. This work is a culmination of years of effort and discussion between neuroimaging researchers and MRI methods developers around the globe. Our extension will not only aid in organizing qMRI data, but will also facilitate multi-center collaborative work, encourage neuroscientists to adapt advanced MR techniques and go a long way toward the standardization of qMRI methods.

Results

A new BIDS common principle: entity-linked file collections. The majority of qMRI methods necessitate the grouping of a set of similar images where specific acquisition parameters are carefully varied. Furthermore, the images that are collected for qMRI application do not usually have a clear “weighting” description (e.g., T1w, T2w), unlike the conventional structural images. The novel concept of file collections decouples the semantics of logical group identification from contrast weighting labels or acquisition sequence names that are not originally developed for qMRI (e.g., FLASH). Instead, suffixes for such logical units may indicate a generic MRI readout type (e.g., multi-echo gradient echo: MEGRE), a qMRI sequence name (e.g., magnetization prepared two rapid gradient echoes, MP2RAGE) or a qMRI data collection framework (e.g., variable flip angle, VFA). Table 1 lists file collection suffixes for various qMRI and fieldmap data, and the quantitative parameters they can derive. These suffixes span a wide range of qMRI applications including relaxometry, MT imaging, multiparametric mapping, and RF field mapping. Application scope can be extended without necessarily adding more suffixes. The BIDS qMRI appendix presents a set of rules and suggestions to add new qMRI suffixes to the specification (<https://bids-specification.readthedocs.io>).

Note that the use of file collections is not exclusive to qMRI, anatomy imaging data, or even MRI. Any imaging modality calling for a file grouping logic to define a quantitative or qualitative application can benefit from this principle by specifying a descriptive suffix and filename entity. Such changes would require additional BIDS extensions to create a valid file collection.

To distinguish individual files of a file collection, we introduced filename entities that are associated with commonly altered acquisition parameters (e.g., flip angle) or with inherent components of the same data (e.g., phase information), hence the name “entity-linked file collection” (Table 2).

It is important to highlight that these entities cannot store acquisition parameter values in the filename but can only index or categorize them. Respective parameter values are stored in so-called “sidecar JSON”-files.

qMRI application	Suffix	Derived maps	BIDS folder	Reference
Magnetization prepared two rapid gradient echoes (MP2RAGE)	MP2RAGE	T1	anat	Marques <i>et al.</i> 2010 ⁵⁸
Multiparametric mapping (MPM)	MPM	T1, T2*, PD, MT	anat	Weiskopf <i>et al.</i> 2013 ³²
Variable flip angle (VFA)	VFA	T1, T2	anat	Gupta <i>et al.</i> 1997 ¹²
Inversion recovery for T1 mapping (IRT1)	IRT1	T1	anat	Barral <i>et al.</i> 2010 ⁶⁵
Multi-echo spin-echo (MESE)	MESE	T2, MWF	anat	Carr and Purcell 1954 ⁶⁶ , Mackay <i>et al.</i> 1994 ⁶⁷
Multi-echo gradient-echo (MEGRE)	MEGRE	T2*	anat	Ma and Wehrli 1996 ⁶⁸
Magnetization transfer ratio (MTR)	MTR	MT _%	anat	Wolff <i>et al.</i> 1989 ⁶⁹
Magnetization transfer saturation index (MTS)	MTS	MT _{sat}	anat	Helms <i>et al.</i> 2008 ⁷⁰
Double angle B1 + mapping	TB1DAM	B1+	fmap	Insko and Bolinger 1993 ⁷¹
B1 + mapping with 3D echo-planar imaging (EPI)	TB1EPI	B1+	fmap	Jiru and Klose 2006 ⁷²
Actual flip angle imaging (AFI)	TB1AFI	B1+	fmap	Yarnykh 2007 ⁷³
Rapid B1 + mapping with TurboFLASH readout	TB1TFL	B1+	fmap	Chung <i>et al.</i> 2010 ⁷⁴
Saturation-prepared with 2 rapid gradient echoes (SA2RAGE)	TB1SRGE	B1+	fmap	Eggenschwiler <i>et al.</i> 2012 ⁷⁵
Inter-scan motion correction using receive field modulation	RB1COR	B1-	fmap	Papp <i>et al.</i> 2016 ⁷⁶

Table 1. File collections of anatomy imaging data to derive parametric maps of longitudinal, transverse and observed-transverse relaxation times (T1, T2 and T2*, respectively), proton density (PD), magnetization transfer ratio and saturation index (MTR and MT_{sat}) and myelin water fraction (MWF). Relaxation rates (e.g., T1⁻¹ and T2⁻¹) and residual terms (e.g., M0) are excluded from the table for brevity.

Entity format	Entity values	Associated acquisition parameter	Associated qMRI file collections
echo-<index>	01,02,03,...,n	EchoTime	MEGRE, MESE, MPM
flip-<index>	01,02,03,...,n	FlipAngle	VFA, MTS, MPM
inv-<index>	01,02,03,...,n	InversionTime	IRT1, MP2RAGE
mt-<label>	on/off	MTState	MTR, MTS, MPM
part-<label>	mag/phase	N/A	MP2RAGE

Table 2. Filename entities representing an MRI acquisition parameter or designating an inherent part of the reconstructed image (e.g., magnitude or phase).

Requirement level of these entities in relation to file collections are presented in the BIDS entity table appendix (<https://bids-specification.readthedocs.io/en/stable/99-appendices/04-entity-table.html>).

Data organization for qMRI file collections and quantitative parametric maps. By combining entities in the filename that represent different acquisition parameters (Table 2) with entity-linked file collection suffixes (Table 1), BEP001 provides an intuitive way to organize filenames of most existing qMRI data. For example, raw data from MP2RAGE acquisitions comprises both magnitude and phase reconstructed images, acquired at two successive inversion times (Fig. 1a). The respective file collection for MP2RAGE (Fig. 1b) clearly defines these components via *part* and *inv* entities, which are required for the MP2RAGE file collection. Note how the BIDS inheritance rules do allow for using a single JSON-file to describe both phase and magnitude images, since these have identical acquisition parameters. In addition, the same collection suffix can be extended to specify its multi-echo variant³¹ using the echo entity, which is made optional to MP2RAGE. For clarity, these specific use cases are defined in the BIDS qMRI appendix.

The same logic applies to the raw images of double-angle B1 + mapping, identified by the TB1DAM suffix (Fig. 1a,b). In this case, the maximum value of the flip entity indicates that the data is collected over two flip angles. We recognize that an alternative approach to organize such data is stacking images at each flip angle into the 4th dimension of a NIfTI file and storing the corresponding metadata in vector form using a single JSON file. This approach offers a less crowded file list for this example. However, indexing acquisition parameter dependent variations across additional dimensions is less favourable for comprehensive qMRI methods. For example, MPM³² collects raw data at different echo times, flip angles, and MT preparations with the option of phase reconstruction. After extended debates that took more than a year, the qMRI-BIDS extension group ultimately concluded that this approach is less favourable for human-readability of qMRI datasets, especially for multiparametric acquisition methods where the number of images per protocol can go into the dozens.

Metadata requirements for file collections and quantitative parametric maps. For the file collections, linking entities (Table 2) indicate a requirement for the respective acquisition parameters that are subject to change from image-to-image. Therefore, the entity table appendix lists such parameters as required in relation to the corresponding file collection suffix based on the descriptions made in the BIDS schema. Note that not all the parameters that change across file collection images are captured by a linking entity but may still be required

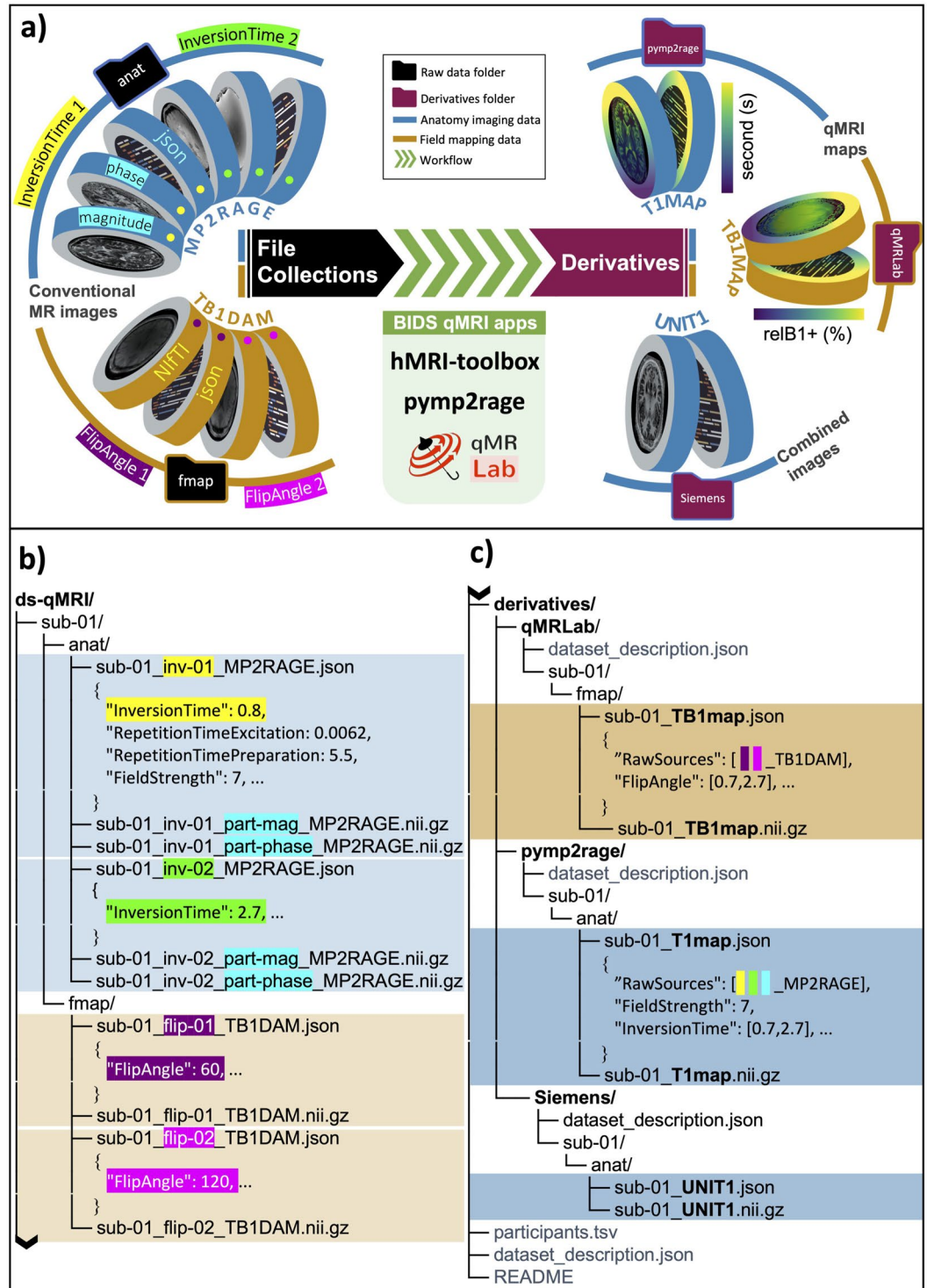


Fig. 1 (a) Schematic representation of BIDS formatted raw (left) and derived (right) quantitative MRI (qMRI) data. MP2RAGE (anat) and TB1DAM (fmap) file collections highlight entity-linked metadata fields for the *InversionTime* (yellow and green), the *FlipAngle* (purple and pink), and for the reconstructed image type (cyan). Derivatives from these file collections are generated by using *pympr2rage* and *qMRLab*, yielding T1 and B1+ maps. (b) File organization of raw qMRI data for MP2RAGE and TB1DAM file collections, where respective linking entities are highlighted for the *inv* entity (yellow and green, *InversionTime*), the *flip* entity (purple and pink, *FlipAngle*) and the *part* entity (cyan, magnitude/phase). (c) File organization of qMRI derivatives indicating how sidecar JSON files of quantitative maps generated by open-source software keeps a log of the input files (the *BasedOn* field) and associated acquisition parameters (*FlipAngle* in TB1map and *InversionTime* in B1map).

for data fitting. For example, the value of the *FlipAngle* parameter might (but does not necessarily) covary with that of *InversionTime* between MP2RAGE file pairs; however, the filenames are distinguished solely by the *inv* entity (since that is the crucial parameter that is swept over, whereas the flip angle could in principle remain the same). In addition, certain parameters that are constant across file collection images may be required as well. For example, *RepetitionTimeExcitation* and *RepetitionTimePreparation* are required metadata for an MP2RAGE acquisition. Such parameters are required when they are strictly necessary to calculate the qMRI-maps that a specific acquisition scheme was designed to obtain, e.g., a T1-map in case of MP2RAGE. BEP001 added an array of new metadata fields that may be required for certain file collections (e.g., *MTState*, specifying whether an MT preparation is enabled in an MPM acquisition, associated with the *mt* linking entity) or provide supporting information (e.g., *SpoilingRFPhaseIncrement*, specifying the amount of incrementation applied to the phase of an excitation pulse). The complete list of metadata fields and their requirement levels for all the qMRI file-collections are included in the BIDS release v1.5.0 and later. Currently, metadata conversions for some of these required fields have been implemented in *dcm2niix*³³, a commonly used DICOM to NIfTI converter to create BIDS-compatible datasets.

Certain quantitative parameters cannot be interpreted in absence of fundamental scanner specifications. For example, to interpret relaxometry maps (e.g., T1map), the magnetic field strength must be known. The BEP001 ensures that such requirements are met (please see the qMRI Appendix in BIDS release v1.5.0 and later). Moreover, sidecar JSON files of quantitative maps contain all the metadata values involved in the fitting by representing varying parameters in vector form and inheriting the constant ones from the raw images. To supplement the provenance recording of parameter estimation process with software-relevant details, the derived dataset and pipeline rules are respected as outlined in the modality agnostic files section of the main specification.

Finally, the units and range of the fitted parameters have been standardized by BEP001 to define interchangeable qMRI maps. For relaxometry-based parameters (e.g., T1map or T2map), the time is described in seconds and the rate in reciprocal seconds or Hz. Wherever applicable, unitless ratio maps are described in percentage (e.g., MTRmap or MWFmap). For quantitative susceptibility maps (i.e., Chimap) the local magnetic susceptibility is represented in parts per million. The RF transmit maps (i.e., TB1map) are specified in relative percentage units, where 100% denotes the ideal case (i.e., measured flip angle equals the nominal value). Any deviations from 100% convey proportional deviations from the intended field strength. Please note that certain quantitative parameters are described in arbitrary units, where the acceptable range of values vary based on the target anatomy (e.g., MTsat).

Community software for qMRI-BIDS data acquisition, conversion, and processing. As of release v1.5.0, the BIDS validator can perform on BEP001-compatible qMRI data at the directory and filename level rules, based on the entity requirement levels specified per file collection suffix. However, metadata-level validation rules have not been implemented yet. This is mainly because multi-vendor extraction of qMRI related metadata fields (e.g., *MTState* or *RepetitionTimePreparation*) is not supported by commonly used converters. Recently, we started working with *dcm2niix*³³ and *BIDSme* (<https://github.com/CyclotronResearchCentre/bidsme>) developers to identify and map vendor-specific header information to BEP001 compatible metadata.

Discussion

Even though vendor-native DICOM headers satisfy most of the requirements for conventional imaging, they lack some metadata entities that are of profound importance to the accuracy of quantitative maps. For example, the BIDS fields of *RFSpoilingPhaseIncrement* and *SpoilingGradientMoment* are two major determinants of T1 and B1+ estimation accuracy using spoiled gradient echo based applications³⁴. Although this information is not provided by vendors, open-source pulse sequence development frameworks such as *Pulseseq*³⁵, *PyPulseseq*³⁶, *Gammastar*³⁷, *TOPPE*³⁸, *SequenceTree*³⁹, *ODIN*⁴⁰ and *RTHawk*⁴¹ can make a qMRI-tailored metadata annotation possible. An example implementation is the vendor-neutral sequences (VENUS) study, showing that open-source pulse sequences that export data in the qMRI-BIDS format can improve multi-center reproducibility of qMRI⁴². Therefore, we highly encourage open-source MRI pulse sequence developers to use and contribute to the qMRI metadata annotations. This simple consensus can remove proprietary roadblocks from disseminating qMRI datasets that incorporate key information on the reproducibility of data acquisition.

Most qMRI methods can benefit from a plethora of BIDS applications⁴ to prepare data for parameter estimation and downstream statistical analyses. There are several open-source tools emerging to perform qMRI fitting at multiple levels, like the *hMRI-toolbox*⁴³, *qMRLab*⁴⁴, *QUIT*⁴⁵, *PyQMRI*⁴⁶, *QMRTools*⁴⁷, *mrQ*⁴⁸, *Madym*⁴⁹, *MITK-ModelFit*⁵⁰, *ROCKETSHIP*⁵¹, *DCEMRI.jl*⁵² and *DCE@urLAB*⁵³. Giving these tools the ability to operate on BIDS formatted data is an important step towards establishing interoperable qMRI processing pipelines.

The role of BIDS in wider adoption, accessibility and standardization of quantitative MRI. Quantitative MRI offers a rapidly developing set of techniques that can inform us about brain (micro) structure beyond what conventional MRI techniques have to offer⁵⁴. We believe that, in coming years, qMRI will become increasingly important to both clinical and fundamental brain science. Therefore, a concrete standard for organizing and thereby also disseminating open qMRI data sets is much warranted. BEP001 extends the framework of the existing and widely used BIDS standard, to develop a standard for qMRI in the form of a “BIDS extension proposal”. To aid actual user adoption of this standard, it includes very precise descriptions of how to use it in many real-life qMRI use-cases, as well as many example data sets.

Currently, obtaining qMRI data is still expensive and needs considerable expertise, which is not readily available at many MRI facilities. Therefore, we also hope that BEP001 will aid researchers that do not have easy access

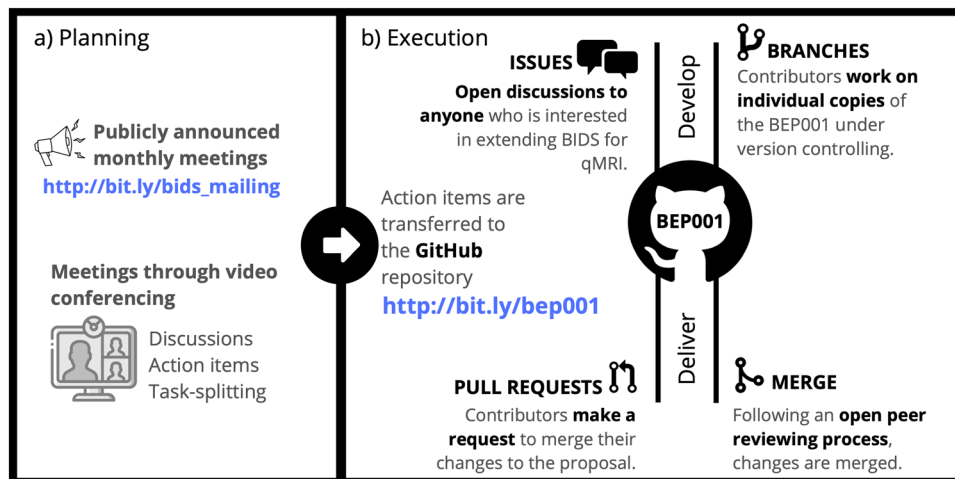


Fig. 2 Summary of the standard operational procedure for improving BEP001. Outcomes from the monthly meetings (a) are transferred to a central GitHub repository, opened for more elaborate public discussions via issues and merged into the proposal through peer-reviewed pull requests (b). BEP001 is inclusive to all communities who would like to contribute to the proposal or keep themselves up to date with the latest developments.

to such facilities to get familiar with qMRI data and potentially can even use open qMRI data sets for their research questions.

The popularity of BIDS is likely in large part also due to some software packages that are designed around this standard and therefore extremely easy-to-use, when one's data adheres to the BIDS standard²⁵. We hope that the success of BIDS in the domain of functional MRI will also inspire and encourage MRI software developers to work on similar “BIDS apps” to make it easier to work with qMRI data, as well as make processing pipelines more open and transparent.

Quantitative MRI is in a dire need of standardization from scanner to the publication⁵⁶ of integrated research objects⁵⁷ to reach its full potential. The data standard developed by the present work provides an important stepping stone towards achieving this wider objective.

Methods

Community-driven development of BEP001. The development history of BEP001 spanned nearly 5 years. This extension was initiated by a mailing list discussion about standardizing MP2RAGE⁵⁸ datasets and supporting multi-echo MRI acquisitions in the main specification (https://bit.ly/bids_mailing). These discussions revealed that BIDS was lacking a generic convention to specify structural acquisitions yielding multiple contrasts. In the summer of 2018, two meetings were held to hear concerns and questions from interested participants, and to set an action plan for the development during: i) the annual INCF NeuroInformatics conference in Montréal/Canada (<http://www.neuroinformatics2018.org/>) and ii) the OHBM meeting in Singapore (<https://www.humanbrainmapping.org/i4a/pages/index.cfm?pageID=3821>). As the first action, a joint-community meeting was organized between MRI and neuroimaging scientists on 4 October 2018 (<https://www.ismrm.org/virtual-meetings/virtual-meetings-archive/>), where a consensus decision was made on extending the specification for a variety of qMRI methods. After this meeting, BEP001 was migrated to GitHub to centralize and organize the development tasks under version control. This enabled establishing a standard operational procedure to advance the proposal by focusing on both transparency and accessibility to other researchers (Fig. 2).

Following a year of development via online meetings (see Fig. 2 for an illustration of its procedure), BIDS incorporated and released BEP001 as part of their version 1.5.0. The main problems identified and resolved during the development are outlined in the following section, laying out the methodology of how qMRI can be incorporated into BIDS.

Extending an existing standard for new use cases. BIDS traditionally focused on conventional anatomical images that are collected in functional MRI experiments and whose contrast characteristics are well-defined (i.e., mostly T1-weighted images). This posed a challenge for the naming scheme of collections of multimodal images used in qMRI. Unlike conventional structural imaging data, qMRI inputs are usually formed by collections of images where specific acquisition parameters are systematically manipulated. As a result, the standard weighting labels (e.g., T1, T2w etc.) cannot clearly define the differences between the contrast characteristics of these images. A concrete example: in a multi-echo GRE acquisition with a long TRs, early echoes will be mostly PD- and B1+/-B1 – signal-weighted, whereas later echoes will be increasingly T2*-weighted. Most echoes will show a contrast that is the result of a mixture of underlying physical properties. This ambiguity renders MRI weightings (e.g., T1w or T2starw) unsuitable as suffix labels to specify interchangeable qMRI datasets. In addition, the use of proprietary acquisition sequence names like “FLASH” (fast low angle shot) or “GRE” (gradient-recalled echo) as a suffix is not suitable either. This is because different MRI vendors use different naming conventions

and one type of sequence can often be used for numerous qMRI applications. To address this problem, BEP001 introduced a new common principle: file collections.

A second challenge that BEP001 addressed pertains to standardizing the data organization of quantitative parametric maps. One central challenge of such maps is that the calculations on which they are based can be made both by proprietary vendor software run on the scanner system, or offline using open-source workflows. The resultant map can be described as derivative data in either case, yet the former lacks provenance of the whole calculation process and may not export the raw inputs to the calculation.

Data availability

The example dataset we created by converting publicly available qMRI data into the developed BIDS format can be found at the OSF repository⁵⁹. Other third-party datasets are included in the spine generic project⁶⁰, the neuromod project⁶¹, the vendor-neutral sequences (VENUS) study⁶² and the hMRI-toolbox software⁶³.

Code availability

Source code to generate quantitative maps in the example dataset are provided by qMRLab⁴⁴, hMRI-Toolbox⁴³ and pypm2rage⁶⁴. Each software provides extensive user documentation, which were followed to create derivative datasets.

Received: 28 October 2021; Accepted: 19 July 2022;

Published online: 24 August 2022

References

- Gorgolewski, K. J. *et al.* The brain imaging data structure, a format for organizing and describing outputs of neuroimaging experiments. *Scientific data* **3**, 1–9, <https://doi.org/10.1038/sdata.2016.44> (2016).
- Markiewicz, C. J. *et al.* OpenNeuro: An open resource for sharing of neuroimaging data. *bioRxiv*, 2021.2006.2028.450168, <https://doi.org/10.1101/2021.06.28.450168> (2021).
- Poldrack, R. *et al.* Toward open sharing of task-based fMRI data: the OpenfMRI project. *Frontiers in Neuroinformatics* **7**, 12 (2013).
- Gorgolewski, K. J. *et al.* BIDS apps: Improving ease of use, accessibility, and reproducibility of neuroimaging data analysis methods. *PLoS computational biology* **13**, e1005209 (2017).
- Esteban, O. *et al.* MRIQC: Advancing the automatic prediction of image quality in MRI from unseen sites. *PLoS one* **12**, e0184661 (2017).
- Esteban, O. *et al.* fMRIPrep: a robust preprocessing pipeline for functional MRI. *Nature methods* **16**, 111–116 (2019).
- Inati, S. J. *et al.* ISMRM Raw data format: A proposed standard for MRI raw datasets. *Magnetic resonance in medicine* **77**, 411–421, <https://doi.org/10.1002/mrm.26089> (2017).
- Hansen, M. S. & Sørensen, T. S. Gadgetron: an open source framework for medical image reconstruction. *Magnetic resonance in medicine* **69**, 1768–1776, <https://doi.org/10.1002/mrm.24389> (2013).
- Maier, O. *et al.* CG-SENSE revisited: Results from the first ISMRM reproducibility challenge. *Magnetic resonance in medicine* **85**, 1821–1839, <https://doi.org/10.1002/mrm.28569> (2021).
- Wilkinson, M. D. *et al.* The FAIR Guiding Principles for scientific data management and stewardship. *Scientific data* **3**, 1–9 (2016).
- Novikov, D. S., Kiselev, V. G. & Jespersen, S. N. On modeling. *Magn Reson Med* **79**, 3172–3193, <https://doi.org/10.1002/mrm.27101> (2018).
- Gupta, R. K. A new look at the method of variable nutation angle for the measurement of spin-lattice relaxation times using fourier transform NMR. *Journal of Magnetic Resonance* **25**, 231–235, [https://doi.org/10.1016/0022-2364\(77\)90138-X](https://doi.org/10.1016/0022-2364(77)90138-X) (1977).
- Stikov, N., Trzasko, J. D. & Bernstein, M. A. Reproducibility and the future of MRI research. *Magnetic Resonance in Medicine* **82**, 1981–1983, <https://doi.org/10.1002/mrm.27939> (2019).
- Lundervold, A. S. & Lundervold, A. An overview of deep learning in medical imaging focusing on MRI. *Zeitschrift für Medizinische Physik* **29**, 102–127 (2019).
- Golkov, V. *et al.* Q-space deep learning: twelve-fold shorter and model-free diffusion MRI scans. *IEEE transactions on medical imaging* **35**, 1344–1351 (2016).
- Yoo, Y. *et al.* Deep learning of joint myelin and T1w MRI features in normal-appearing brain tissue to distinguish between multiple sclerosis patients and healthy controls. *NeuroImage: Clinical* **17**, 169–178 (2018).
- Lyu, Q. & Wang, G. Quantitative MRI: absolute T1, T2 and proton density parameters from deep learning. *arXiv preprint arXiv:1806.07453* (2018).
- Wu, Y., Ma, Y., Du, J. & Xing, L. Accelerating quantitative MR imaging with the incorporation of B1 compensation using deep learning. *Magnetic Resonance Imaging* **72**, 78–86 (2020).
- Bojorquez, J. Z. *et al.* What are normal relaxation times of tissues at 3 T. *Magn Reson Imaging* **35**, 69–80, <https://doi.org/10.1016/j.mri.2016.08.021> (2017).
- Weinberger, D. R. & Radulescu, E. Finding the Elusive Psychiatric “Lesion” With 21st-Century Neuroanatomy: A Note of Caution. *American Journal of Psychiatry* **173**, 27–33, <https://doi.org/10.1176/appi.ajp.2015.15060753> (2015).
- Lorio, S. *et al.* Neurobiological origin of spurious brain morphological changes: A quantitative MRI study. *Human brain mapping* **37**, 1801–1815 (2016).
- Draganski, B. *et al.* Regional specificity of MRI contrast parameter changes in normal ageing revealed by voxel-based quantification (VBQ). *Neuroimage* **55**, 1423–1434 (2011).
- Lommers, E. *et al.* Voxel-Based Quantitative MRI reveals spatial patterns of grey matter alteration in multiple sclerosis. *Human Brain Mapping* **42**, 1003–1012, <https://doi.org/10.1002/hbm.25274> (2021).
- Weiskopf, N., Mohammadi, S., Lutti, A. & Callaghan, M. F. Advances in MRI-based computational neuroanatomy: from morphometry to *in-vivo* histology. *Current opinion in neurology* **28**, 313–322 (2015).
- Weiskopf, N., Callaghan, M. F., Josephs, O., Lutti, A. & Mohammadi, S. Estimating the apparent transverse relaxation time (R2*) from images with different contrasts (ESTATICS) reduces motion artifacts. *Frontiers in neuroscience* **8**, 278 (2014).
- Lutti, A., Dick, F., Sereno, M. I. & Weiskopf, N. Using high-resolution quantitative mapping of R1 as an index of cortical myelination. *Neuroimage* **93**, 176–188 (2014).
- Haast, R. A. M., Ivanov, D. & Formisano, E. & Uludağ, K. Reproducibility and reliability of quantitative and weighted T1 and T2* mapping for myelin-based cortical parcellation at 7 Tesla. *Frontiers in neuroanatomy* **10**, 112 (2016).
- Dinse, J. *et al.* A cytoarchitecture-driven myelin model reveals area-specific signatures in human primary and secondary areas using ultra-high resolution *in-vivo* brain MRI. *Neuroimage* **114**, 71–87 (2015).
- Mancini, M. *et al.* An interactive meta-analysis of MRI biomarkers of myelin. *eLife* **9**, <https://doi.org/10.7554/elife.61523> (2020).

30. Lazari, A. & Lipp, I. Can MRI measure myelin? Systematic review, qualitative assessment, and meta-analysis of studies validating microstructural imaging with myelin histology. *Neuroimage*, 117744, <https://doi.org/10.1016/j.neuroimage.2021.117744> (2021).
31. Caan, M. W. A. *et al.* MP2RAGEME: T1, T2*, and QSM mapping in one sequence at 7 tesla. *Human brain mapping* **40**, 1786–1798 (2019).
32. Weiskopf, N. *et al.* Quantitative multi-parameter mapping of R1, PD(*), MT, and R2(*) at 3T: a multi-center validation. *Front Neurosci* **7**, 95, <https://doi.org/10.3389/fnins.2013.00095> (2013).
33. Li, X., Morgan, P. S., Ashburner, J., Smith, J. & Rorden, C. The first step for neuroimaging data analysis: DICOM to NIfTI conversion. *Journal of neuroscience methods* **264**, 47–56 (2016).
34. Yarnykh, V. L. Optimal radiofrequency and gradient spoiling for improved accuracy of T1 and B1 measurements using fast steady-state techniques. *Magnetic Resonance in Medicine* **63**, 1610–1626, <https://doi.org/10.1002/mrm.22394> (2010).
35. Layton, K. J. *et al.* Pulseq: a rapid and hardware-independent pulse sequence prototyping framework. *Magnetic resonance in medicine* **77**, 1544–1552, <https://doi.org/10.1002/mrm.26235> (2017).
36. Ravi, K. S., Geethanath, S. & Vaughan, J. T. PyPulseq: A python package for mri pulse sequence design. *Journal of Open Source Software* **4**, 1725 (2019).
37. Cordes, C., Konstantin, S., Porter, D. & Günther, M. Portable and platform-independent MR pulse sequence programs. *Magnetic resonance in medicine* **83**, 1277–1290, <https://doi.org/10.1002/mrm.28020> (2020).
38. Nielsen, J. F. & Noll, D. C. TOPPE: A framework for rapid prototyping of MR pulse sequences. *Magnetic resonance in medicine* **79**, 3128–3134, <https://doi.org/10.1002/mrm.26990> (2018).
39. Magland, J. F., Li, C., Langham, M. C. & Wehrli, F. W. Pulse sequence programming in a dynamic visual environment: SequenceTree. *Magnetic resonance in medicine* **75**, 257–265, <https://doi.org/10.1002/mrm.25640> (2016).
40. Jochimsen, T. H. & Von Mengershausen, M. ODIN—object-oriented development interface for NMR. *Journal of Magnetic Resonance* **170**, 67–78, <https://doi.org/10.1016/j.jmr.2004.05.021> (2004).
41. Santos, J. M., Wright, G. A. & Pauly, J. M. In *The 26th Annual International Conference of the IEEE Engineering in Medicine and Biology Society*. 1048–1051 (2004).
42. Karakuzu, A., Biswas, L., Cohen-Adad, J. & Stikov, N. Vendor-neutral sequences and fully transparent workflows improve inter-vendor reproducibility of quantitative MRI. *Magnetic Resonance in Medicine* **88**, 1212–1228, <https://doi.org/10.1002/mrm.29292> (2022).
43. Tabelow, K. *et al.* hMRI—A toolbox for quantitative MRI in neuroscience and clinical research. *Neuroimage* **194**, 191–210 (2019).
44. Karakuzu, A. *et al.* qMRLab: Quantitative MRI analysis, under one umbrella. *Journal of Open Source Software* **5**, 2343, <https://doi.org/10.21105/joss.02343> (2020).
45. Wood, T. C. QUIT: QUantitative imaging tools. *Journal of Open Source Software* **3**, 656 (2018).
46. Maier, O., Spann, S. M., Bödenler, M. & Stollberger, R. PyQMRI: an accelerated Python based quantitative MRI toolbox. *Journal of Open Source Software* **5**, 2727 (2020).
47. Froeling, M. QMRTools: a Mathematica toolbox for quantitative MRI analysis. *Journal of Open Source Software* **4**, 1204 (2019).
48. Mezer, A. *et al.* Quantifying the local tissue volume and composition in individual brains with magnetic resonance imaging. *Nature medicine* **19**, 1667–1672 (2013).
49. Berks, M. m Parker, G. J., Little, R. & Cheung, S. Madym: A C++ toolkit for quantitative DCE-MRI analysis. *Journal of Open Source Software* **6**, 3523 (2021).
50. Debus, C. *et al.* MITK-ModelFit: A generic open-source framework for model fits and their exploration in medical imaging—design, implementation and application on the example of DCE-MRI. *BMC bioinformatics* **20**, 1–18 (2019).
51. Barnes, S. R. *et al.* ROCKETSHP: a flexible and modular software tool for the planning, processing and analysis of dynamic MRI studies. *BMC medical imaging* **15**, 1–20 (2015).
52. Smith, D. S., Li, X., Arlinghaus, L. R., Yankeelov, T. E. & Welch, E. B. DCEMRI.jl: a fast, validated, open source toolkit for dynamic contrast enhanced MRI analysis. *PeerJ* **3**, e909 (2015).
53. Ortuño, J. E. *et al.* DCE@ urLAB: a dynamic contrast-enhanced MRI pharmacokinetic analysis tool for preclinical data. *BMC bioinformatics* **14**, 1–17 (2013).
54. Weiskopf, N., Edwards, L. J., Helms, G., Mohammadi, S. & Kirilina, E. Quantitative magnetic resonance imaging of brain anatomy and *in vivo* histology. *Nature Reviews Physics* **3**, 570–588, <https://doi.org/10.1038/s42254-021-00326-1> (2021).
55. Yarkoni, T. *et al.* PyBIDS: Python tools for BIDS datasets. *Journal of open source software* **4** (2019).
56. Niso, G. *et al.* Open and reproducible neuroimaging: from study inception to publication. *OSF Preprints* <https://doi.org/10.31219/osf.io/pu5vb> (2022).
57. DuPre, E. *et al.* Beyond advertising: New infrastructures for publishing integrated research objects. *PLOS Computational Biology* **18**, e1009651, <https://doi.org/10.1371/journal.pcbi.1009651> (2022).
58. Marques, J. P. *et al.* MP2RAGE, a self bias-field corrected sequence for improved segmentation and T1-mapping at high field. *Neuroimage* **49**, 1271–1281, <https://doi.org/10.1016/j.neuroimage.2009.10.002> (2010).
59. Karakuzu, A. *et al.* qMRI-BIDS example dataset. *Open Science Framework* <https://doi.org/10.17605/osf.io/k4bs5> (2021).
60. Cohen-Adad, J. *et al.* Spine Generic Public Database (Multi-Subject). *Zenodo* <https://doi.org/10.5281/zenodo.4299139> (2020).
61. Bellec, P. & Boyle, J. Bridging the gap between perception and action: the case for neuroimaging, AI and video games. <https://doi.org/10.31234/osf.io/3epws> (2019).
62. Karakuzu, A., Cohen-Adad, J. & Stikov, N. Multicenter VENUS dataset: Comparing vendor-neutral and vendor-native MTsat acquisitions. *Open Science Framework* <https://doi.org/10.17605/osf.io/5n3cu> (2022).
63. Callaghan, M. F. *et al.* Example dataset for the hMRI toolbox. *Data in Brief* **25**, 104132, <https://doi.org/10.1016/j.dib.2019.104132> (2019).
64. de Hollander, G. Gilles86/pymp2rage: First alpha version pymp2rage. *Zenodo* <https://doi.org/10.5281/zenodo.1476976> (2018).
65. Barral, J. K. *et al.* A robust methodology for *in vivo* T1 mapping. *Magnetic resonance in medicine* **64**, 1057–1067 (2010).
66. Carr, H. Y. & Purcell, E. M. Effects of diffusion on free precession in nuclear magnetic resonance experiments. *Physical review* **94**, 630 (1954).
67. MacKay, A. *et al.* *In vivo* visualization of myelin water in brain by magnetic resonance. *Magn Reson Med* **31**, 673–677 (1994).
68. Ma, J. & Wehrli, F. W. Method for image-based measurement of the reversible and irreversible contribution to the transverse-relaxation rate. *Journal of Magnetic Resonance, Series B* **111**, 61–69 (1996).
69. Wolff, S. D. & Balaban, R. S. Magnetization transfer contrast (MTC) and tissue water proton relaxation *in vivo*. *Magnetic resonance in medicine* **10**, 135–144 (1989).
70. Helms, G., Dathe, H. & Dechent, P. Quantitative FLASH MRI at 3T using a rational approximation of the Ernst equation. *Magn Reson Med* **59**, 667–672, <https://doi.org/10.1002/mrm.21542> (2008).
71. Insko, E. K. & Bolinger, L. Mapping of the radiofrequency field. *Journal of Magnetic Resonance, Series A* **103**, 82–85 (1993).
72. Jiru, F. & Klöse, U. Fast 3D radiofrequency field mapping using echo-planar imaging. *Magnetic Resonance in Medicine* **56**, 1375–1379, <https://doi.org/10.1002/mrm.21083> (2006).
73. Yarnykh, V. L. Actual flip-angle imaging in the pulsed steady state: a method for rapid three-dimensional mapping of the transmitted radiofrequency field. *Magn Reson Med* **57**, 192–200 (2007).
74. Chung, S., Kim, D., Breton, E. & Axel, L. Rapid B1+ mapping using a preconditioning RF pulse with TurboFLASH readout. *Magnetic resonance in medicine* **64**, 439–446 (2010).

75. Eggenschwiler, F., Kober, T., Magill, A. W., Gruetter, R. & Marques, J. P. SA2RAGE: A new sequence for fast B1+-mapping. *Magnetic resonance in medicine* **67**, 1609–1619 (2012).
76. Papp, D., Callaghan, M. F., Meyer, H., Buckley, C. & Weiskopf, N. Correction of inter-scan motion artifacts in quantitative R1 mapping by accounting for receive coil sensitivity effects. *Magnetic resonance in medicine* **76**, 1478–1485 (2016).

Acknowledgements

The authors would like to acknowledge the work by other contributors to BIDS, and those who contributed to BEP-001 via the Github repository, intermediate meetings, as well as a first draft on Google Drive. For BEP-001, recorded contributions include those from Suyash Bhogawar, Julien Cohen-Adad, Elizabeth Dupre, Chris Gorgolewski, Daniel Handwerker, Michael Harms, Ilana Leppert, Tobias Leutritz, Dylan Nielson, Julien Sein, Isla Staden, Wietske van der Zwaag, and Tobias Wood. This research was funded in part by the Wellcome Trust [Grant 109062/Z/15/Z to AL]. For Open Access, the author has applied a CC BY public copyright licence to any Author Accepted Manuscript version arising from this submission. TA's work has been funded by the Biotechnology and Biological Sciences Research Council, London (BB/S008314/1). C.P. is supported by the F.R.S.-FNRS, Belgium. G.H. was funded by a Rubicon grant from the Dutch Research Council (NWO). A.K. is supported by \Canada First Research Excellence Fund through the TransMedTech Institute, Canadian Open Neuroscience Platform (CONP) and International Society for Magnetic Resonance in Medicine (ISMRM).

Author contributions

A.K., G.H. and K.W. prepared the original manuscript; A.K., G.H. and K.W. developed the initial draft of the standard and managed community contributions. A.K. merged the extension proposal to the main BIDS specification. G.H. and K.W. supervised the project. A.K., S.A., T.A., M.B., F.F., A.K., A.L., C.M., M.M., C.P., T.S., N.S., K.W. and G.H. contributed to meetings and drafts outlining the extension proposal. A.K., S.A., T.A., M.B., F.F., A.K., A.L., C.M., M.M., C.P., T.S., N.S., K.W. and G.H. revised the original manuscript.

Competing interests

The authors declare no competing interests.

Additional information

Correspondence and requests for materials should be addressed to A.K., K.W. or G.d.H.

Reprints and permissions information is available at www.nature.com/reprints.

Publisher's note Springer Nature remains neutral with regard to jurisdictional claims in published maps and institutional affiliations.



Open Access This article is licensed under a Creative Commons Attribution 4.0 International License, which permits use, sharing, adaptation, distribution and reproduction in any medium or format, as long as you give appropriate credit to the original author(s) and the source, provide a link to the Creative Commons license, and indicate if changes were made. The images or other third party material in this article are included in the article's Creative Commons license, unless indicated otherwise in a credit line to the material. If material is not included in the article's Creative Commons license and your intended use is not permitted by statutory regulation or exceeds the permitted use, you will need to obtain permission directly from the copyright holder. To view a copy of this license, visit <http://creativecommons.org/licenses/by/4.0/>.

© The Author(s) 2022